ISSN 0023-1584, Kinetics and Catalysis, 2008, Vol. 49, No. 2, pp. 305–312. © MAIK "Nauka/Interperiodica" (Russia), 2008.
Original Russian Text © P.M. Eletskii, V.A. Yakovlev, V.V. Kaichev, N.A. Yazykov, V.N. Parmon, 2008, published in Kinetika i Kataliz, 2008, Vol. 49, No. 2, pp. 321–328.

Texture and Surface Properties of Carbon–Silica Nanocomposite Materials Prepared by the Carbonization of High-Ash Vegetable Raw Materials in a Fluidized Catalyst Bed

P. M. Eletskii, V. A. Yakovlev, V. V. Kaichev, N. A. Yazykov, and V. N. Parmon

Boreskov Institute of Catalysis, Siberian Branch, Russian Academy of Sciences, Novosibirsk, 630090 Russia
e-mail: yeletsky@catalysis.ru

Received October 10, 2006

Abstract—A series of carbon–silica nanocomposite samples prepared by the carbonization of high-ash biomass (using rice husks as an example) in a fluidized-bed reactor with a deep oxidation catalyst at 450–600°C was studied by a set of physicochemical techniques (BET, IR spectroscopy, XPS, and TGA). The dependence of the chemical composition, texture characteristics, and main properties of the resulting materials on carbonization temperature was found.

DOI: 10.1134/S0023158408020201

INTRODUCTION

Agriculture is a large-scale source of biomass as a sufficiently homogeneous chemical raw material. The high ash content of some types of these raw materials can be used successfully for the production of carbon-mineral composites. Rice husks are most interesting in this respect. The world's resources of rice husks as large-tonnage waste from rice milling are as high as 100 million tons annually (about 20% of paddy rice weight). In Russia, rice husks are formed as a large-tonnage resource in Krasnodar krai; the amount of this resource is 140000–150000 ton per year; only about 20% of this amount finds further use, primarily, as low-grade fuel. Indeed, the use of rice husks as fuel in standard boiler equipment is associated with the problem of a low calorific value of this fuel because of a high ash content (to 20 wt %). On the other hand, the high silica content of rice husks allows one to use rice husks as an inexpensive and homogeneous starting material for the production of valuable silicon compounds such as SiC; Si_3N_4; pure SiO_2, Si, and $SiCl_4$; zeolites; liquid glass; cement; and other widely used silicon-containing compounds [1–7]. In this connection, intensive studies are under way in order to develop efficient processes for rice husk conversion into highly marketable products [3, 7]. The pyrolysis of rice husks for the production of volatile organic compounds (a mixture of phenols, organic acids, and alcohols) and silicon–carbon materials (amorphous carbon and silica (SiO_2)) is considered as the most promising process [3, 8–11].

Processes performed in the fluidized beds of solid heat-transfer materials occupy a special place among the thermal methods of rice husk conversion for the simultaneous manufacture of gaseous and liquid products of pyrolysis [12] and carbon-mineral composites [13]. An oxidative treatment process (combustion or gasification) performed in an apparatus with the fluidized bed of solid heat-transfer material provides an opportunity to control purposefully many process parameters: the temperature, the contact time, and the ratio of atmospheric oxygen to fuel carbon. In turn, this allows one to affect the rate and degree of carbonization of rice husks and to obtain carbon-mineral composites with various properties.

Generally, a process of the oxidative treatment (carbonization) of rice husks in a fluidized bed with a contact time (τ) shorter than 1 s can be considered in terms of the generalized reaction scheme

$$C_{3.3}H_5O_2 \cdot (SiO_2)_n + O_2$$

$$\longrightarrow CO_2 + CO + \text{volatile organic compounds}$$

$$+ \text{ash residue.}$$

In this reaction scheme, the ash residue is carbonized silicon dioxide (C/SiO_2).

The aim of this work was to obtain nanocomposite carbon-mineral materials by the carbonization of rice husks at relatively low temperatures in a fluidized-bed reactor with a deep oxidation catalyst and to study the structure and morphology of the resulting samples in order to find their characteristic properties and possible areas of application. The chosen process for the carbonization of rice husks combined a high rate of the process (the contact time was $\tau \sim 1$ s) and the possibility of performing the process in the autothermal mode with controllable process temperature.

Table 1. Composition of the parent rice husks (according to Koz'mina [14]) and the ash residue (obtained by ICP AES) based on elemental analysis data

Elemental composition of the parent rice husks, wt %		Elemental composition of the ash residue, wt %	
C	41.50	K_2O	2.17
H	5.50	Na_2O	0.3
O	33.2	CaO	1.06
N	0.05	MgO	0.33
S	0.02	Al_2O_3	0.11
Cl	0.01	ZnO	0.007
Ash residue	19.50	Mn_2O_3	0.08
		Fe_2O_3	0.12
		CuO	0.02
		Cr_2O_3	0.01
		SiO_2	95.78

EXPERIMENTAL

Preparation of Carbon-Mineral Composites

Rice husks (Krasnodar krai) with the following characteristics were used: husk length, 8–10 mm; width, 2–3 mm; thickness, 0.1–0.15 mm. The moisture content was about 5 wt % (TGA). According to published data [14], the lignin, cellulose, and hemicellulose contents of the test rice husks from Krasnodar krai were 19–25, 34–42, and 17–22%, respectively. Table 1 summarizes the elemental analysis data for the rice husks and ash residue. The rice husks were preground to obtain a fraction with a particle size of 1 mm or smaller.

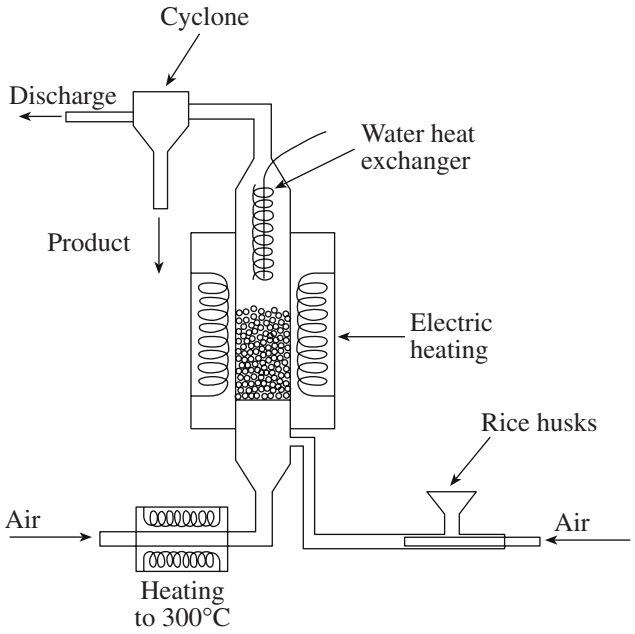

Fig. 1. Schematic diagram of the catalytic fluidized-bed reactor.

A fluidized-bed steel reactor 40 mm in i.d. and 1200 mm in height with an IC-12-73 deep oxidation catalyst (from OAO Katalizator) with a particle size of 2–3 mm was used for the carbonization of rice husks. The catalyst consisted of CuO + MgO + Cr_2O_3 (10–15 wt %) supported on γ-Al_2O_3; the $CuCr_2O_4/MgCr_2O_4$ ratio was 1 : 1 by weight. The use of this catalyst allowed us to oxidize completely the gaseous products of rapid rice husk pyrolysis at lower temperatures without the formation of CO and other toxic compounds.

The rice husks were supplied to the reactor (Fig. 1) with a flow of air (the molar ratio of atmospheric oxygen to rice husk carbon was $\alpha \sim 2$). The carbonization time was $\tau \sim 1$ s. After the carbonization of rice husks in a fluidized bed of the catalyst at a specified temperature, the resulting carbon-mineral material was collected in a cyclone. The carbonization temperatures were 450, 500, 550, and 600°C. The reactor temperature was regulated using electric heating units. At 600°C, the carbonization occurred in the autothermal mode.

Instrumentation

The texture characteristics of samples were measured by the BET method using the physical adsorption of N_2 at 77 K on a Micromeritics ASAP 2400 adsorption instrument (United States).

The chemical composition of sample surfaces was studied on a VG ESCALAB HP electron spectrometer (Vacuum Generators, the United Kingdom) using AlK_α radiation ($h\nu$ = 1486.6 eV). The scale of binding energies (E_b) was precalibrated using the Au $4f_{7/2}$ (84.0 eV) and Cu $2p_{3/2}$ (932.67 eV) peak positions in the spectra of gold and copper foils, respectively. The relative concentrations of the elements in the analysis zone (the depth of analysis was 2–3 nm) were determined from the integrated XPS line intensities corrected for atomic sensitivity factors [15].

The IR spectra of samples were measured on a Bomem MB-102 spectrometer (Canada) in the frequency range 4000–200 cm^{-1} with the accumulation of 100 scans. The analytical samples were pressed as pellets with KBr.

A Q-1500 D derivatograph (MOM, Hungary) was used to perform thermogravimetric analysis (TGA). The rate of sample heating from room temperature to 800°C was 10 K/min. The sample weight was 100 mg. Platinum labyrinth crucibles, which were blown with nitrogen at a flow rate of 25 l/h, were used in the analysis of samples in an inert atmosphere.

Table 2. Texture characteristics of carbon–silica nanocomposites prepared by the carbonization of rice husks in a fluidized-bed reactor at 450–600°C according to BET data

Fluidized bed temperature, °C	S_{BET}, m^2/g	V_Σ, cm^3/g	V_μ, cm^3/g	Average pore size, nm	Ash content, %
450	32	0.04	~0	5.3	35
500	176	0.15	0.03	2.6	56
550	246	0.21	0.05	2.6	69
600	233	0.22	0.04	2.8	76

Note: S_{BET} is the specific surface area, V_Σ is the total pore volume, and V_μ is the micropore volume.

The ash residue of rice husks was analyzed by inductively coupled plasma atomic emission spectrometry (ICP AES) on a Perkin-Elmer Optima 4300 instrument (United States). The analytical procedure was published elsewhere [16].

RESULTS AND DISCUSSION

Commonly used processes for the production of carbon-mineral composites like C/SiO_2 and C/Al_2O_3 are based on the thermal or thermocatalytic decomposition of gaseous or liquid hydrocarbons on a mineral matrix [17–19]. The advantage of rice husks as a starting material for the production of a carbon–silica composite is that rice husks initially contain both carbon and mineral components. Data in Table 1 indicate that the total ash content of the rice husks used was almost 20 wt % and the ash residue mainly consisted of SiO_2. Along with silicon dioxide, alkali and alkaline earth metal compounds and the oxides of Al, Fe, Zn, and Cr were the constituents of the ash residue.

Composites prepared by the carbonization of rice husks in a fluidized catalyst bed contain carbon and silica phases, which likely occur in a dispersed state on a nanolevel. The high dispersity of the two phases can be explained by the fact that a silica-containing phase is uniformly distributed in the lignocellulose matrix of the parent rice husks [20], and these phases stabilize each other upon carbonization to remain in a dispersed state at relatively low temperatures.

The process used in this study for the carbonization of rice husks in a fluidized catalyst bed is easy to perform, and it allows one to widely vary the characteristics of the resulting products. Thus, Table 2 summarizes the texture characteristics of the carbon–silica composites prepared by the carbonization of rice husks at various working temperatures in a catalyst bed.

It can be seen that the degree of combustion of the carbon phase increased with temperature (the ash content of the final sample increased). At the same time, the values of S_{BET}, V_Σ, and V_μ of the resulting nanocomposites exhibited maximums at $T = 550$°C. Evidently, the surface of the composites was developed because of the rapid gasification of the starting biomass; in this case, the gasification temperature was responsible for the intensity of this process. It is likely that the low porosity of a composite prepared at 450°C ($S_{BET} = 32$ m^2/g; $V_\Sigma = 0.04$ cm^3/g) suggests that the gasification and carbonization processes were incomplete at this temperature and the sample contained a considerable amount of undecomposed lignocellulose residues.

To study the nature and surface properties of the resulting carbon–silica composites, we used IR spectroscopy and XPS.

Figure 2 shows the survey IR spectra of the resulting nanocomposite samples. All of the spectra exhibited four main regions of sample absorption at 3400, 1650, 1100, and 460 cm^{-1}. The absorption region at 3400 cm^{-1} was related to the presence of hydroxyl groups and chemisorbed water on the surface [21]. An intense absorption peak at 1080 cm^{-1} and a peak in the region of 1200 cm^{-1} can be attributed to siloxane groups like Si–O–Si. A peak at 2930 cm^{-1} suggested the presence of a certain amount of C–H groups that remained from the starting rice husks on the carbon surface. As the fluidized-bed temperature was increased, the peak inten-

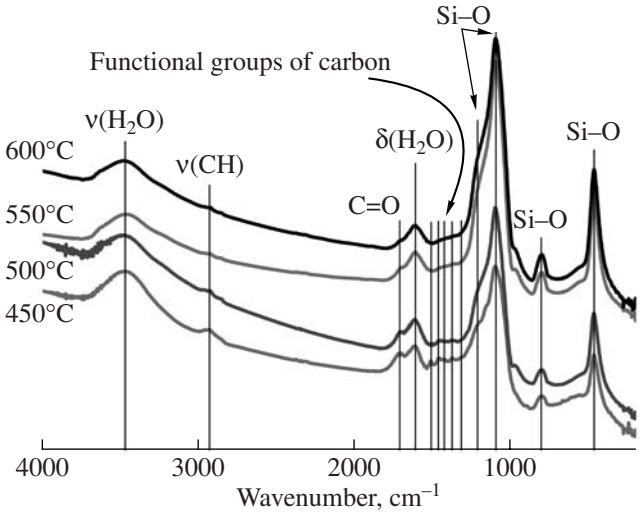

Fig. 2. IR spectra of samples prepared by the carbonization of rice husks at 450–600°C.

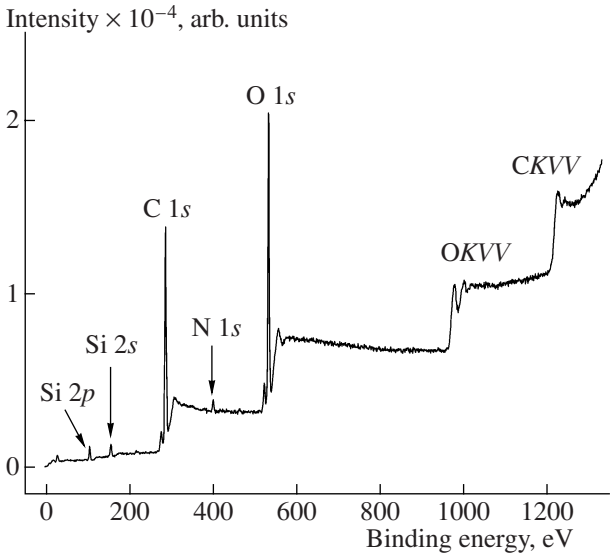

Fig. 3. Survey XPS spectrum of the starting rice-husk powder.

sity at 2930 cm^{-1} decreased; this fact suggested the elimination of surface carbon species containing C–H units. In this case, oxidized carbon species with absorption at 1710, 1620, and 1450 cm^{-1} occurred in larger amounts. We attributed absorption at 1710 and 1620 cm^{-1} to C=O vibrations in ketone and aldehyde groups, respectively. A low-intensity broad peak at 1450 cm^{-1} corresponded to C–O bond vibrations in the carbonyl group. The relative intensities of peaks at 1710, 1620, and 1450 cm^{-1} remained unchanged as the temperature of carbonization was increased. It is believed that the formation of oxidized surface carbon species in the fluidized-bed carbonization of rice husks under the specified conditions occurred by either (1) the thermal degradation of initial cellulose, hemicellulose, and lignin fragments with the formation of surface ketone, aldehyde, and carboxyl groups or (2) the oxidation of the carbon surface with the surface oxygen of the catalyst with the formation of analogous groups.

At a carbonization temperature of 450°C, it is likely that oxygen-containing functional groups were formed by the former reaction path because rice husk lignin, which is the source of these groups, had no time to decompose completely. The latter reaction path predominated at higher carbonization temperatures. However, in this case, the total contribution of both of the reaction paths was constant because, as can be seen in Fig. 2, the concentration of surface functional groups remained almost unchanged with temperature.

We used XPS to study the composition of the near-surface layers of parent rice husks and a series of C/SiO_2 samples prepared at 450, 500, 550, and 600°C. Figure 3 shows a survey XPS spectrum of the parent rice husks. It can be seen that the spectra exhibited lines due to silicon and nitrogen in addition to the intense lines of oxygen and carbon. Thus, the photoemission of electrons from the C 1*s* level of carbon was responsible for an intense line at 285 eV. The photoemission of electrons from the O 1*s* level of oxygen was responsible for a peak at 533 eV. Less intense lines at 103, 155, and 399 eV corresponded to the photoemission of electrons from the Si 2*p*, Si 2*s*, and N 1*s* levels, respectively. In addition, the spectra exhibited the O*KVV* and C*KVV* Auger lines at 980 and 1230 eV, respectively [15]. Table 3 summarizes the relative concentrations of the elements Si, C, O, and N in the near-surface regions of the samples, as determined from XPS data. Insignificant concentrations of K, Ca, and Mg were also detected in all of the samples.

Figure 4 shows the characteristic C 1*s*, Si 2*p*, and O 1*s* XPS spectra of the test samples. Four lines at 282.5, 284.4, 286.0, and 287.8 eV can be distinguished in the C 1*s* XPS spectra (Fig. 4a). According to published data, the most intense line at 284.4 eV corresponds to the C–C/C–H fragments of a carbon matrix. Lines with greater binding energies correspond to carbon chemically bound to oxygen [22–25]. As a rule, C 1*s* lines in the region 286.0–286.3 eV are attributed to alcohol or ether groups. For ketone and carbonyl groups, the C 1*s* binding energy is 287.0–287.8 eV. Carboxyl groups are characterized by a much higher C 1*s* binding energy (288.4–289.1 eV). A weak shoulder in the region of lower binding energies (283 eV) suggests the occurrence of carbon atoms chemically bound to silicon [26–28].

Table 3. Relative atomic concentrations of oxygen, carbon, silicon, and nitrogen and the ash content of the surface region of the parent rice husks and carbon–silica composite samples prepared at various temperatures, as determined from XPS data

T, °C	[O]/[Si]	[O]/[C]	[C]/[Si]	[N]/[C]	Ash content according to XPS, %	Bulk ash content, %
Parent rice husks	4.9	0.38	15	0.026	23	19
450	3.9	0.63	6.1	0.014	40	35
500	2.6	0.84	3.1	0.027	59	56
550	2.3	1.20	1.9	0.025	70	69
600	2.1	1.30	1.7	0.026	74	76

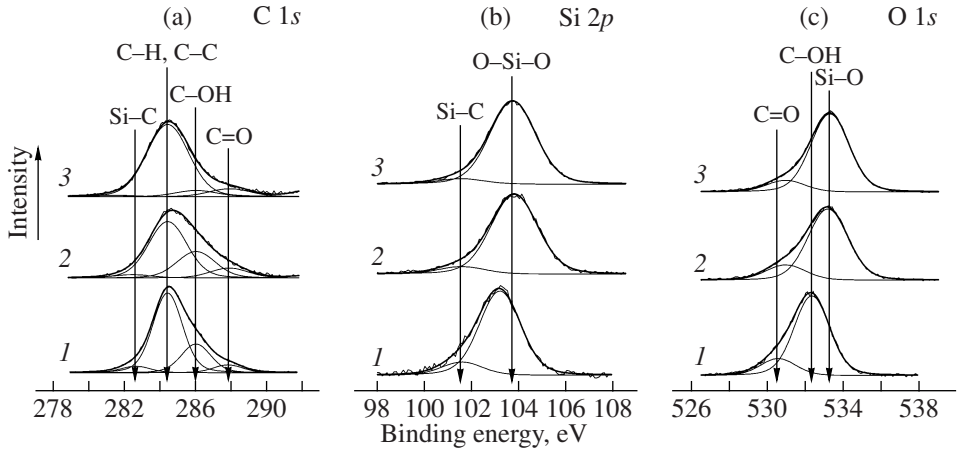

Fig. 4. (a) C 1*s*, (b) Si 2*p*, and (c) O 1*s* XPS spectra of (*1*) the parent rice husks and the samples prepared at (*2*) 450 and (*3*) 600°C.

In the Si 2*p* XPS spectrum of the parent rice husks (Fig. 4b), an intense line at 103.2 eV was observed; the position of this line corresponds to silicon as a constituent of SiO_x fragments [28, 29]. A weak shoulder in the region of lower binding energies (~102 eV) suggests the occurrence of Si–C fragments [26–28]. For carbonized rice husk samples, the Si 2*p* binding energy is 103.7 eV, which suggests the formation of a SiO_2 phase [29]. Indeed, in the course of carbonization, on the one hand, a portion of carbon was removed to increase the ash content of the samples, whereas, on the other hand, the [O]/[Si] atomic ratio decreased (Fig. 5). Thus, the [O]/[Si] atomic ratio in the parent rice husks was 4.9, which indicated that the major portion of oxygen as a constituent of the rice husks entered into the organic component (Table 3). It can also be seen that the bulk ash content of the samples was almost equal to the surface ash content, which was determined using XPS. The surface ash content was calculated with the use of the [O]/[Si] and [C]/[Si] atomic ratios, which were found by XPS, from the equation

$$\text{Ash content} = \frac{M(SiO_2)}{[C]/[Si]M(C) + ([O]/[Si] - 2)M(O) + M(SiO_2)} \times 100.$$

Here, M is the molar weight of the corresponding element or compound specified in parentheses. In this case, we assumed that oxygen was bound to silicon in an atomic ratio of 2 : 1 (SiO_2) and the nitrogen content could be ignored (because it was negligible).

A comparative analysis of the bulk and surface ash contents (Table 3) allowed us to conclude that the silica and carbon phases were homogeneously distributed over the nanocomposite grain. A somewhat inhomogeneous distribution of silica was observed in the parent rice husks; in this case, the silica content was somewhat shifted to the surface. This can be explained by the natural structure of rice husks, which serve as the hard protecting coverings of rice grains.

The O 1*s* XPS spectrum exhibited two lines at 530.6 and 532.4 eV (Fig. 4c). The former less intense line corresponded to ketone and carbonyl groups, whereas the latter corresponded to alcohol or ether groups [23]. In a sample prepared at 600°C, the [O]/[Si] surface atomic ratio was 2.1 (Table 3). Moreover, the O 1*s* XPS spectrum exhibited an intense line at 533.2 eV, which is

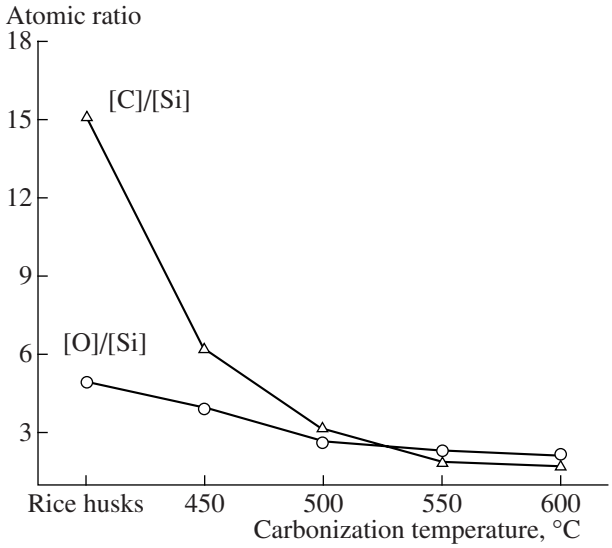

Fig. 5. Dependence of the relative atomic concentrations of C, O, and Si in the surface regions of the parent rice husks and the resulting samples on the temperature of carbonization.

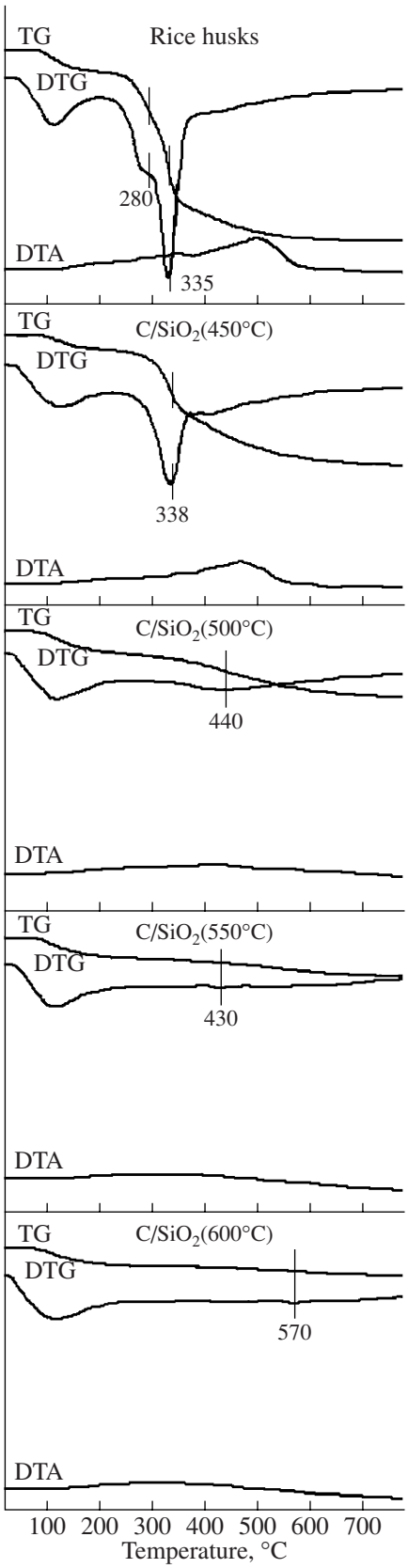

Fig. 6. TGA spectra of the parent rice husks and carbon-mineral composites prepared at various temperatures.

characteristic of an amorphous SiO_2 phase [29]. Thus, the carbonization of rice husks in a fluidized catalyst bed resulted in the removal of oxidized fragments and the graphitization of a carbon matrix. In accordance with XPS data, the removal of alcohol and ether groups (C 1*s* and O 1*s* lines at 286.0 and 532.4 eV, respectively) occurred most intensely. Simultaneously, an increase in the carbonization temperature also resulted in the complete oxidation of silicon with the formation of a SiO_2 phase. This is evidenced by a considerable decrease in the relative intensities of Si 2*p* and C 1*s* lines corresponding to Si–C fragments. The N 1*s* line in the survey XPS spectrum occurred at 399 eV, which corresponds to nitrogen chemically bound to carbon.

To study the constituents of the resulting nanocomposites, we examined the test samples by TGA in an inert atmosphere (Fig. 6). The nature and concentrations of some thermal degradation products of rice husks and the carbon–silica composites prepared from these rice husks were determined from TG, DTG, and DTA spectra (Table 4).

It is well known that the parent rice husks contained carbon as hemicellulose, cellulose, and lignin, which have their own temperatures at which maximum rates of degradation were attained. Indeed, the TGA spectrum of the parent rice husks demonstrated that the decomposition of hemicellulose occurred simultaneously with the removal of physisorbed water in the range 120–200°C. The maximum degradation of cellulose and lignin was observed at 280 and 335°C, respectively. The samples prepared at 450 and 500°C contained two carbon species, which can be classified as undecomposed lignin and soot, respectively. As the carbonization temperature was increased, the concentration of lignin fragments in the composites decreased and the samples prepared at 550 and 600°C did not contain the above carbon species. An insignificant decrease in the weight of these samples in the course of analysis was likely due to the fact that oxygen-containing functional groups of the carbon surface were removed as CO; CO_2; and, probably, simple organic compounds.

Thus, in the carbonization of rice husks in the presence of air in a fluidized-bed reactor with an IK 12-73 catalyst at 450 and 500°C, lignin was oxidized incompletely and the degradation of its fragments was observed in TGA spectra (Fig. 6). In the samples prepared by the carbonization of rice husks at 550 and 600°C, carbon mainly occurred as soot, the surface of which contained a large amount of oxygen-containing functional groups.

Table 4. Thermogravimetric analysis data for the parent rice husks and carbon–silica composites

TGA data	Parent rice husks	Carbonization temperature, °C			
		450	500	550	600
Temperature range of weight loss, °C	to 600	to 700	to 700	to 600	to 600
H_2O_{ads}, wt %	7 (125°C)*	4 (125°C)	6 (120°C)	5.4 (120°C)	4 (125°C)
Volatile substances, wt %	14 (280°C)	18 (335°C)	4 (420°C)	–	–
	31 (335°C)				
Soot, wt %	32 (440°C)	50 (410°C)	39 (430°C)	29.6 (425°C)	22 (400°C)
SiO_2 (ash residue), wt %	19	35	56	69	76

* The temperatures at which maximum rates of weight losses of the specified C/SiO_2 components were attained are specified in parentheses.

CONCLUSIONS

The above study indicates that the short-time carbonization of rice husks in a fluidized catalyst bed in the presence of air allows one to obtain carbon–silica nanocomposites with various texture characteristics and ratios between carbon and silica phases.

Considerable amounts of oxygen-containing groups, including hydroxyl, ketone, aldehyde, and carboxyl groups, were identified on the surface of the resulting composites with the use of XPS and IR spectroscopy. In addition, a comparative analysis of bulk and surface ash contents allowed us to conclude that the distribution of silica and carbon phases within the composites was homogeneous. The high degree of dispersion of one phase in the other is responsible for a high phase interface, which can be effectively used for the synthesis of silicon compounds such as Si, SiC, silicates, and chlorosilanes.

The concentration of undecomposed lignin fragments in the composite can be changed by varying the temperature of carbonization. These fragments can play both a negative and a positive role in the subsequent processing of the resulting materials, for example, in the course of steam or steam–air gasification, pyrolysis, and topochemical synthesis.

ACKNOWLEDGMENTS

This work was supported by the "Support to Leading Scientific Schools" program (grant no. 6526.2006.3).

REFERENCES

1. Chakraverty, A., Mishra, P., and Banerjee, H.D., *J. Mater. Sci.*, 1988, vol. 23, p. 21.
2. Della, V.P., Kuhn, I., and Hotza, D., *Mater. Lett.*, 2002, vol. 57, p. 818.
3. Sun, L. and Gong, K., *Ind. Eng. Chem. Res.*, 2001, vol. 40, no. 25, p. 5861.
4. Chen, J.M. and Chang, F.W., *Ind. Eng. Chem. Res.*, 1991, vol. 30, p. 2241.
5. RF Patent 2160707, 1998.
6. Nehdi, M., Duquette, J., and El Damatty, A., *Cem. Concr. Res.*, 2003, vol. 33, p. 1203.
7. Chandrasekhar, S., Satyanarayana, K.G., Pramada, P.N., and Raghavan, P., *J. Mater. Sci.*, 2003, vol. 38, p. 3159.
8. Ganesh, A., Grover, P.D., and Iyer, P.V.R., *Fuel*, 1992, vol. 71, no. 8, p. 889.
9. Song, L.K., Wang, H.P., Lin, C.-J., and Juch, C.-I., *Fuel Process. Technol.*, 1998, vol. 55, no. 3, p. 185.
10. Williams, P.T. and Nugranad, N., *Energy*, 2000, vol. 25, no. 6, p. 493.
11. Islam, M.N. and Ani, F.N., *Bioresour. Technol.*, 2000, vol. 73, p. 67.
12. Albina, D.O., *Energy Sources*, 2003, vol. 25, p. 893.
13. Simonov, A.D., Mishenko, T.I., Yazykov, N.A., and Parmon, V.N., *Chem. Sustainable Dev.*, 2003, vol. 11, p. 277.
14. Koz'mina, E.P., *Ris i ego kachestvo* (Rice and Its Quality), Moscow: Kolos, 1976.
15. Wagner, C.D., Riggs, W.M., Davis, L.E., and Moulder, J.F., *Handbook of X-ray Photoelectron Spectroscopy*, Eden Prairie, Minn.: Perkin-Elmer, 1978.
16. Thompson, M. and Walsh, J.N., *A Handbook of Inductively Coupled Plasma Spectrometry*, Glasgow: Blackie, 1983.
17. Stuart, B., *Modern Infrared Spectroscopy*, Chichester: Wiley, 1996.
18. Mahy, J., Jenneskens, L.W., Grabandt, O., Venema, A., and van Houwelingen, G.D.B., *Surf. Interface Anal.*, 1994, vol. 21, p. 1.
19. Yue, Z.R., Jiang, W., Wang, L., Gardner, S.D., and Pittman, C.U., Jr., *Carbon*, 1999, vol. 37, p. 1785.
20. Dekanski, A., Stevanovic, J., Stevanovic, R., Nikolic, B.Z., and Jovanovic, V.M., *Carbon*, 2001, vol. 39, p. 1195.
21. Rodriguez, N.M., Anderson, P.E., Wootsch, A., Wild, U., Schlögl, R., and Paal, Z., *J. Catal.*, 2001, vol. 197, p. 365.
22. Smirnova, T.P., Badalian, A.M., Yakovkina, L.V., Kaichev, V.V., Bukhtiyarov, V.I., Shmakov, A.N., Asanov, I.P., Rachlin, V.I., and Fomina, A.N., *Thin Solid Films*, 2003, vol. 429, p. 144.

23. Johansson, L.I., Glans, P.-A., Wahab, Q., Grehk, T.M., Eickhoff, Th., and Drube, W., *Appl. Surf. Sci.*, 1999, vol. 150, p. 137.
24. Besling, W.F.A., Goossens, A., Meester, B., and Schoonman, J., *J. Appl. Phys.*, 1998, vol. 83, p. 544.
25. Rodriguez N.M., Anderson, P.E., Wootsch, A., Wild, U., Schlögl, R., and Paal, Z., *J. Catal.*, 2001, vol. 197, p. 365.
26. Smirnova, T.P., Badalian, A.M., Yakovkina, L.V., Kaichev, V.V., Bukhtiyarov, V.I., Shmakov, A.N., Asanov, I.P., Rachlin, V.I., and Fomina, A.N., *Thin Solid Films*, 2003, vol. 429, p. 144.
27. Johansson, L.I., Glans, P.-A., Wahab, Q., Grehk, T.M., Eickhoff, Th., and Drube, W., *Appl. Surf. Sci.*, 1999, vol. 150, p. 137.
28. Besling, W.F.A., Goossens, A., Meester, B., and Schoonman, J., *J. Appl. Phys.*, 1998, vol. 83, p. 544.
29. Khassin, A.A., Yurieva, T.M., Demeshkina, M.P., Kustova, G.N., Itenberg, I.Sh., Kaichev, V.V., Plyasova, L.M., Anufrienko, V.F., Molina, I.Yu., Larina, T.V., Boronovskaya, N.A., and Parmon, V.N., *Phys. Chem. Chem. Phys.*, 2003, vol. 5, p. 4025.